JOURNAL OF CATALYSIS **169,** 510–515 (1997)
ARTICLE NO. CA971707

Nanostructural Evolution of a Pt/CeO_2 Catalyst Reduced at Increasing Temperatures (473–1223 K): A HREM Study

S. Bernal, J. J. Calvino, J. M. Gatica, C. Larese, C. López-Cartes, and J. A. Pérez-Omil

Departamento de Ciencia de los Materiales e Ingeniería Metalúrgica y Química Inorgánica, Facultad de Ciencias, Universidad de Cádiz, Apartado 40, 11510 Puerto Real (Cádiz), Spain

Received January 17, 1997; revised March 20, 1997; accepted March 20, 1997

Experimental HREM combined with computer simulation, digital image processing, and SAED techniques have been fruitfully applied to the nanostructural characterization of a Pt/CeO_2 catalyst reduced at temperatures ranging from 473 to 1223 K. Metal decoration effects were detected upon reduction at 973 K. Alloying phenomena could be observed only at the highest reduction temperatures. The crystallographic analysis of the HREM images shows that $CePt_5$ is the only intermetallic phase present in the catalyst. Likewise, preferential orientation relationships were observed in the growth of the alloy microcrystals on ceria.

INTRODUCTION

Ceria-supported noble metal catalysts are being intensively investigated because of their close relationship with the so-called three way catalysts (TWCs) presently used to purify automotive exhaust emissions (1, 2).

In the specific case of Pt/CeO_2, some earlier studies by Meriaudeau *et al.* (3, 4) have suggested that the formation of a Pt–Ce intermetallic compound plays an important role in determining the deactivation observed upon increasing the reduction temperature from 473 to 773 K. No experimental proof supporting their proposal was given, however. Instead, they refer to the finding by Summers and Ausen (5) who, based on X-ray diffraction (XRD) data, reported the occurrence of Pt–Ce alloying. Nevertheless, the reduction temperature applied in Ref. (5) was much higher: 1173 K. Moreover, the Pt–Ce intermetallic was not identified in their actual catalytic systems, $Pt/CeO_2/Al_2O_3$, being only detected by reducing a physical mixture of Pt and ceria. More recent HREM studies on Pt/CeO_2 reduced at 773 K (6, 7), as well as the TEM investigations of $Pt/CeO_2/SiO_2(Al_2O_3)$ catalysts reduced at 923 K (8, 9), have not provided any evidence for the formation of such intermetallic phase either.

On the other hand, a very recent study (10) on Pt–Ce alloys suggests that, if formed, these alloys might have a significant influence on the chemical and microstructural properties of Pt/CeO_2 catalysts submitted to successive reduction/reoxidation cycles. In effect, according to Ref. (10), Pt/Ce alloys treated with O_2, CO/H_2, and particularly N_2O, lead to Pt/CeO_2 catalysts highly active in CO oxidation. This enhanced activity is interpreted as due to the peculiar microstructure exhibited by the catalysts generated from the alloy oxidation processes.

Our laboratory has been working on the deactivation/regeneration mechanisms operating in ceria-supported rhodium catalysts under a variety of both reducing and oxidizing treatments. In particular, high resolution electron microscopy (HREM) has been systematically applied in this investigation (11–16). Our research project is now extended to Pt/CeO_2 catalysts. The present communication reports on the nanostructural evolution of this system under reducing conditions. Specifically, we shall focus our attention on the experimental conditions leading to the formation of the Pt–Ce intermetallic compound as well as its structural nature. For this purpose, experimental HREM studies are combined with computer simulation, digital image processing, and selected area electron diffraction techniques.

METHODS

The catalyst, $Pt(4\%)/CeO_2$, was prepared by the incipient wetness impregnation technique from an aqueous solution of $[Pt(NH_3)_4](OH)_2$. The ceria sample was a low surface area ($4\ m^2\ g^{-1}$) commercial oxide, 99.9% pure, from Alfa. The impregnated/dried (at 383 K) catalyst precursor was reduced with flowing hydrogen ($60\ cm^3\ min^{-1}$) at a heating rate of $10\ K\ min^{-1}$. The catalyst was held for 1 h at the selected reduction temperature, 473, 623, 773, 973, 1073, and 1173 K, and further evacuated at the reduction temperature for 1 h (except the one reduced at 473 K which was evacuated at 773 K). Also a portion of the sample was reduced at 1223 K for 5 h and evacuated (1 h) at the same temperature. The procedure followed to transfer the catalyst samples into the microscope is reported elsewhere (11). The HREM images were recorded on a JEOL-2000EX microscope with 0.21-nm point resolution. The computer-simulated images

0021-9517/97 $25.00

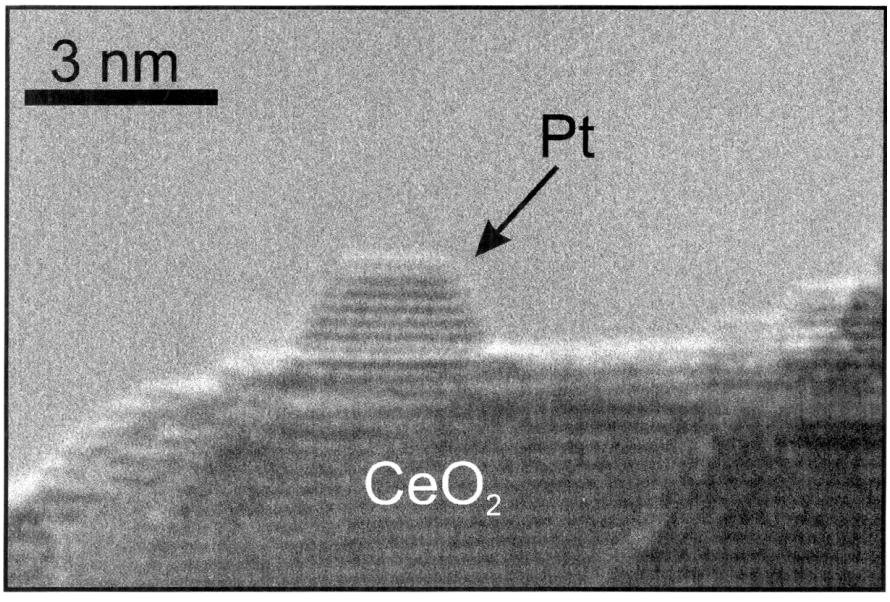

FIG. 1. HREM micrograph recorded on the 4% Pt/CeO_2 catalyst reduced at 773 K. An epitaxial growth of the small platinum particles on ceria can be observed.

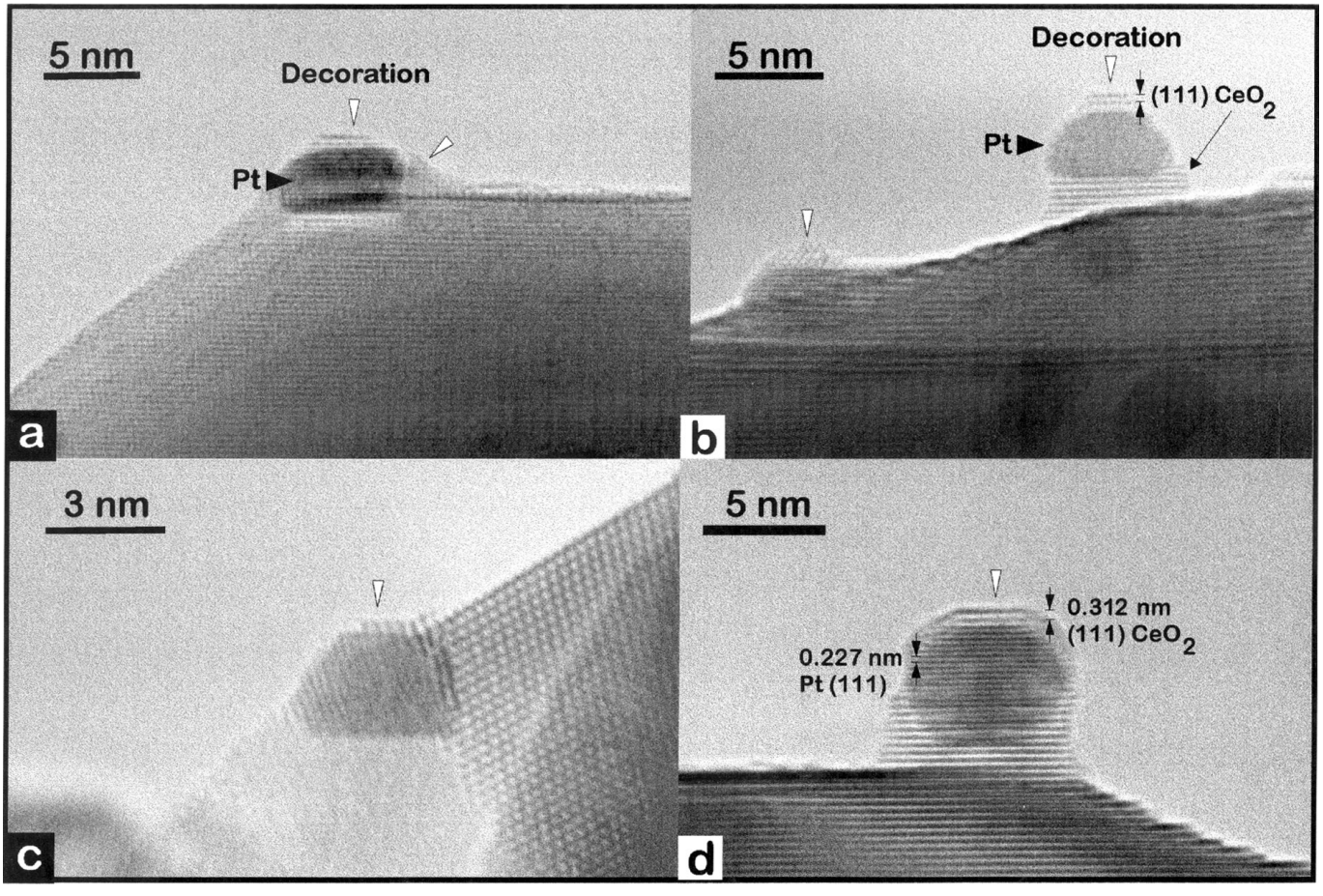

FIG. 2. HREM images corresponding to the 4% Pt/CeO_2 catalyst reduced at 973 K showing the decoration effect. In (a) and (d) a parallel growth of the ceria decorating layers on top of the platinum particles can be noted.

were obtained by running the EMS software package (17) on an Indy 4400SC Silicon Graphics workstation. The experimental micrographs were digitized on a CCD camera, COHU-4910. Digital processing was performed by using the SEMPER 6+ software.

RESULTS AND DISCUSSION

Our HREM study shows that for $T_{redn} \leq 773$ K the Pt microcrystals look like clean and well faceted (Fig. 1). This observation is in good agreement with those reported in Refs. (6, 7) for Pt/CeO_2 catalysts reduced at 773 K. Upon increasing the reduction temperature up to 973 K, metal decoration effects can be noted (Fig. 2). A rather similar effect has already been reported by us for Rh/CeO_2 (11). As in the case of Rh/CeO_2 catalysts, the thin, subnanometric, ceria decoration layers show preferential orientation relationships with respect to the metal particles where they have grown. Note in this respect the parallel alignment between the (111) planes of platinum and the (111) ceria planes in the decorating cap (Figs. 2a and 2d).

Finally, the HREM images recorded on the catalysts reduced at 1073 K (1 h) or 1173 K (1 h) show particles, like those in Figs. 3a and 3b, whose contrasts cannot be interpreted as due to either platinum or ceria. Instead, the 0.46×0.44-nm dot pattern observed in these HREM images can be assigned to the [010] zone axis of a $CePt_5$ phase (Table 1). The 0.46-nm lattice spacing corresponds to that

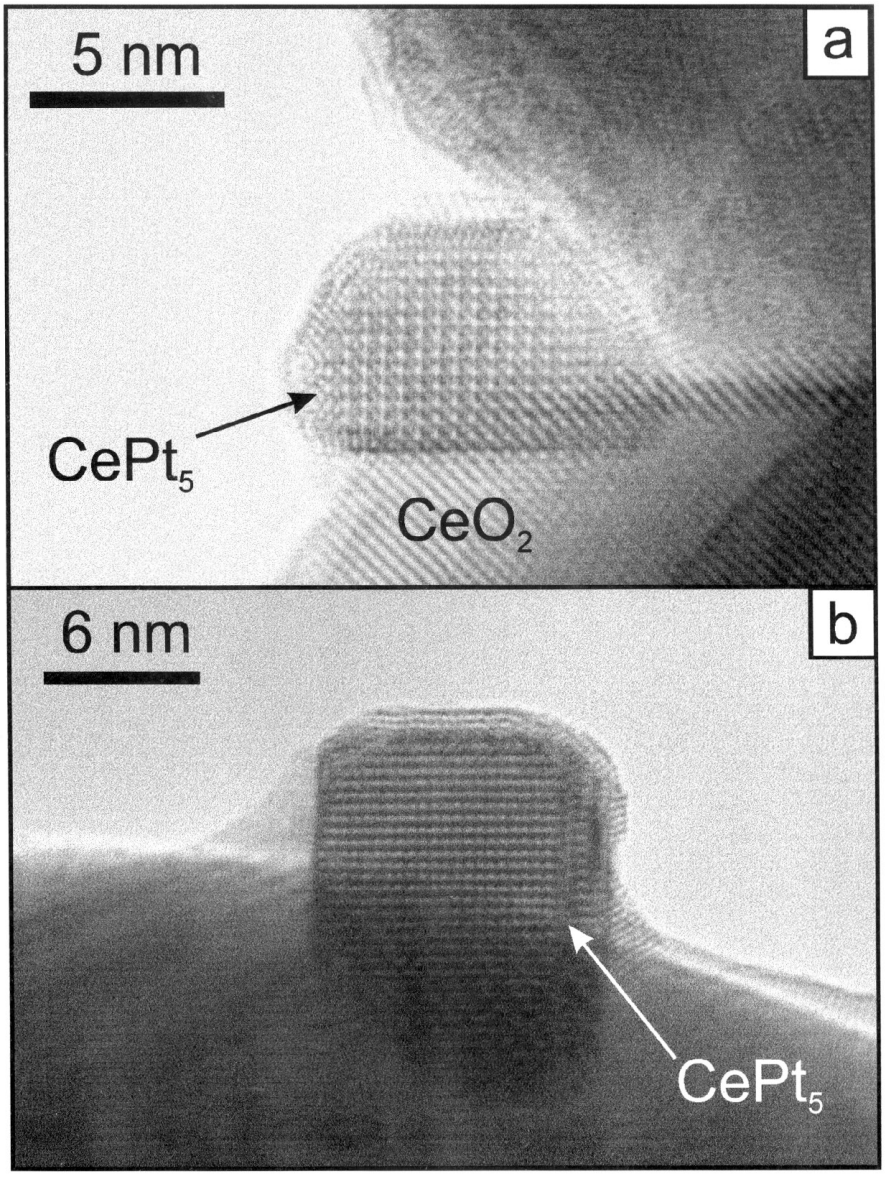

FIG. 3. HREM image corresponding to the 4% Pt/CeO_2 catalyst reduced at 1173 K. $CePt_5$ particles can be identified.

TABLE 1

Geometrical Features of the Zone-Axis HREM Images Characteristic of Each of the Different Intermetallic Pt–Ce Phases Described in the Literature

Phase	Zone axis	$(hkl)_1$	$(hkl)_2$	d_1/nm	d_2/nm	Angle d_1/d_2
$CePt_5$	010	001	100	0.438	0.465	90
CePt	001	110	020	0.369	0.546	70.3
$CePt_2$	001	220	200	0.273	0.386	45
Ce_3Pt_2	$\bar{1}10$	110	003	0.449	0.569	90
Ce_7Pt_3	001	$2\bar{1}0$	110	0.510	0.510	60

of the (100) planes of this intermetallic, whereas that at 0.44 nm should be adscribed to the (001) planes.

This interpretation has been further confirmed by image simulation. Thus, Figs. 4a and 4b account for the calculated images obtained from two structural models of the $CePt_5$ system in [010] orientation. The structural models used as input for these calculations were built up by running the so-called RHODIUS program developed in our laboratory (18). The sample thicknesses considered for these simulations were 6 nm for the image in Fig. 4a and 10 nm in the case of the image in Fig. 4b. To fully match the contrasts observed in the experimental image of Fig. 3a it was necessary to tilt the intermetallic crystal 5° around its (302) plane. The model employed to calculate Fig. 4b corresponded to an in-zone axis, nontilted, $CePt_5$ crystal. As deduced from the comparison of Figs. 3a and 4a, and also Figs. 3b and 4b, a very good agreement is observed between the experimental and calculated HREM images, this result confirming the interpretation suggested above. $CePt_5$ alloy crystallites in $[\bar{1}10]$, [012], and [001] orientations have also been identified from the analysis of our experimental HREM images.

To exclude the likely presence of some other alloy phases, we have performed a systematic crystallographic analysis of the whole series of Pt–Ce intermetallics described in the literature (19–23): CePt, $CePt_2$, Ce_3Pt_2, Ce_7Pt_3, and $CePt_5$. By running the so-called EJE-Z program developed in our laboratory (24), we have established the zone axis for each of these phases allowing to obtain HREM images in our microscope (0.21-nm point resolution). From this study we can also conclude that each of these alloy phases exhibit at least one characteristic zone axis permitting their unequivocal identification in our microscope. Table 1 reports on the crystallographic parameters characterizing these singular zone axis. Having in mind this information, the analysis of tens of experimental micrographs allows us to conclude that no phases other than $CePt_5$ are present in our Pt/CeO_2 catalyst reduced at 1173 K. Likewise, the analysis of such micrographs shows that about 80% of the platinum is in the form of $CePt_5$, the remaining 20% consisting of Pt microcrystals. According to thermodynamic data reported in (25), $CePt_5$ is the most stable Ce–Pt alloy in this range of temperatures, suggesting that, very likely, equilibrium conditions are reached during the treatment in hydrogen for 1 h at high temperature.

The presence of $CePt_5$ has also been confirmed by selected area electron diffraction (SAED). In effect, experimental SAED patterns, like that shown in Fig. 5

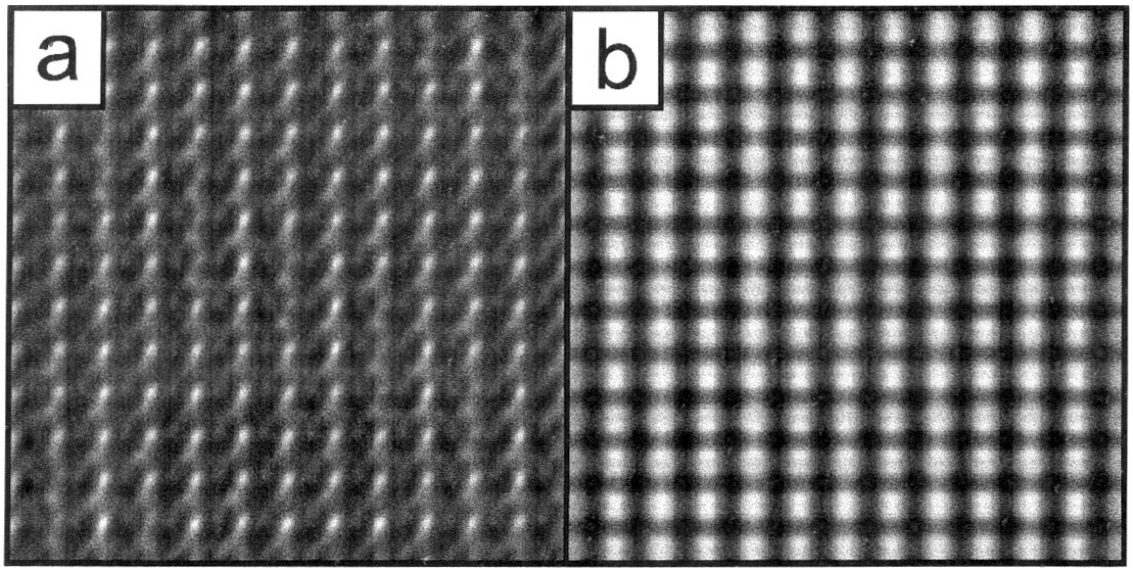

FIG. 4. Image Simulations of the $CePt_5$ phase along the [010] zone axis. In (a) the $CePt_5$ crystal, with a thickness of 6 nm, has been rotated 5° around its (302) plane in order to match the contrasts observed in the experimental image. In (b) an in-zone axis $CePt_5$ crystal of 10 nm thickness has been considered. The value of the electron-optical parameters of these simulations were: Accelerating voltage, 200 KV; objective lens aperture, 12 nm^{-1}; spherical aberration coefficient (C_s), 0.7 mm; beam semiconvergence (θ_c), 1.2 mrad; defocus spread (Δ), 10 nm.

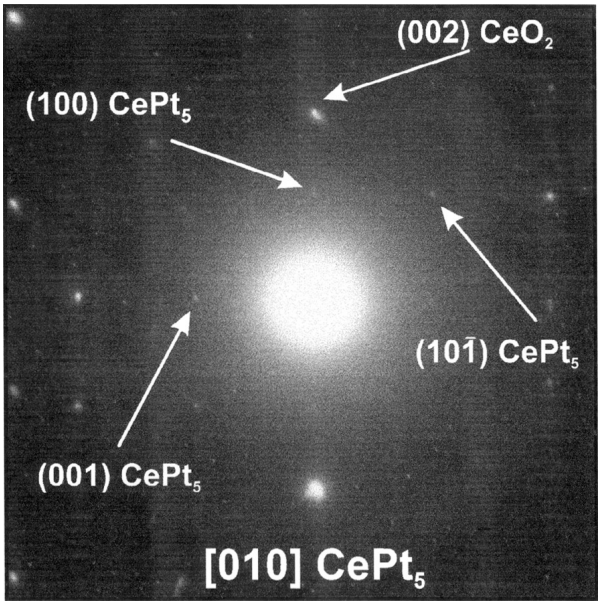

FIG. 5. SAED pattern corresponding to the catalyst 4% Pt/CeO_2 reduced at 1223 K.

corresponding to a sample of the catalyst reduced at 1223 K, show characteristic reflections which can be unambiguously interpreted as due to the hexagonal $CePt_5$ phase.

A further structural feature of the Pt/CeO_2 catalyst reduced at 1223 K worth commenting on is the existence of well-defined orientation relationships between the $CePt_5$ particles and the ceria support. Both the HREM images and the SAED patterns show the occurrence of preferential growth orientations. Specifically we have observed: (a) (100) $CePt_5$//(002) CeO_2, and (b) (001) $CePt_5$//(002) CeO_2. Figure 6 accounts for an example of the former structural relationship. The parallel alignment of the (100) planes of the intermetallic phase with the (002) planes of ceria can be observed in the HREM image (Fig. 6a). The digital diffractogram of the region encircled shows even more clearly such a phenomenon (Fig. 6b). The existence of orientation relationships between ceria and the supported alloy phase might well be a consequence of an epitaxial growth of the intermetallic on the support. The occurrence of epitaxial relationships between Rh and CeO_2 has already been shown (11), in the present case some further studies are needed to confirm such a tentative proposal.

To summarize, experimental HREM combined with computer simulation, digital processing, and SAED techniques has proved to be a useful tool for investigating the nanostructural evolution undergone by a Pt/CeO_2 catalyst reduced at increasing temperatures from 473 to 1223 K. Metal decoration effects were observed upon reduction at 973 K, whereas alloying phenomena could only be detected at the highest reduction temperatures: 1073–1223 K. In contrast to that proposed earlier (3, 4), this suggests that the chemical deactivation effects noted on Pt/CeO_2 catalysts reduced at 773 K can hardly be interpreted in terms of decoration or alloying. Our study has also allowed us to identify the intermetallic phase formed upon high-temperature

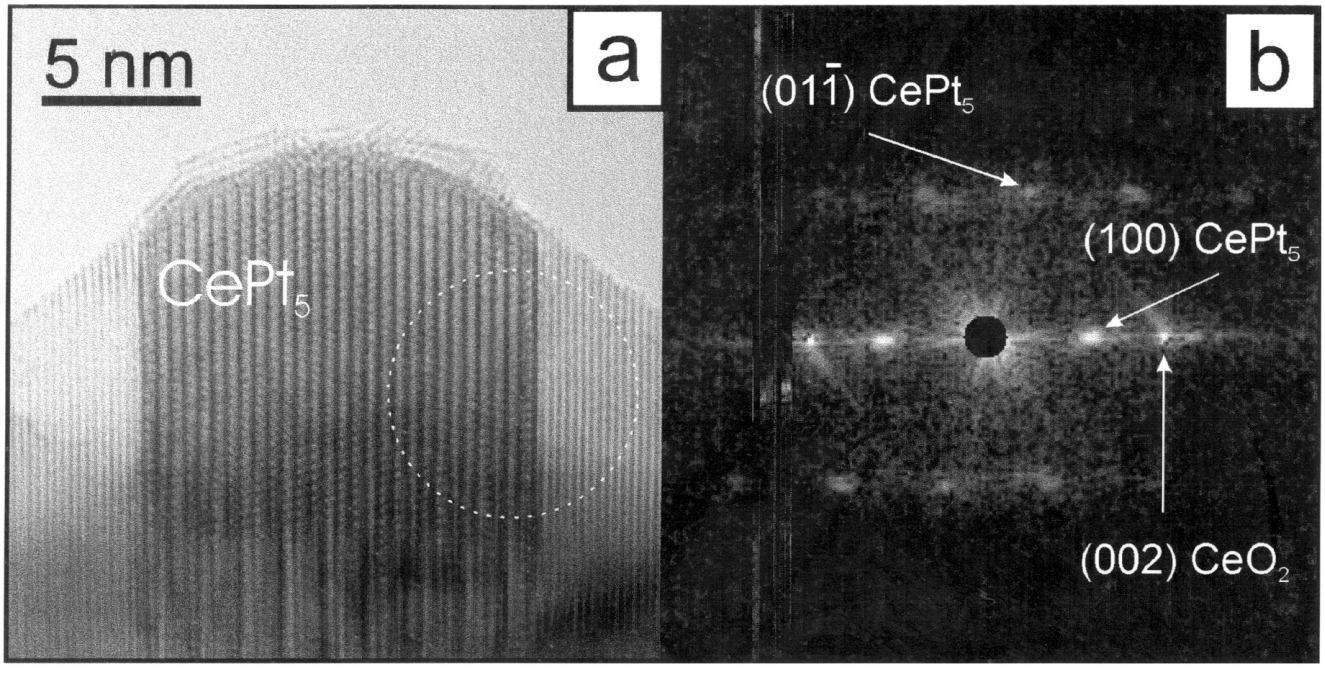

FIG. 6. HREM image (a) and digital diffractogram (b) obtained from the 4% Pt/CeO_2 catalysts reduced at 1223 K.

reduction: $CePt_5$. This phase is the same as that reported by Summers and Ausen (5). Moreover, the crystallographic analysis of the whole series of Pt–Ce alloys shows that $CePt_5$ is the only intermetallic phase present in our catalyst.

ACKNOWLEDGMENTS

This work has been supported by the CICYT (Project No. MAT96-0931) the DGICYT (Project No. PB95-1257) and the Junta de Andalucía. We thank Johson Matthey for a loan of precious metals. The HREM images were obtained at the Electron Microscopy Facilities of Cádiz University (Spain).

REFERENCES

1. Golunski, S., Hatcher, H. A., Rajaram, R. R., and Truex, T. J., *Appl. Catal. B Environ.* **5**, 367 (1995).
2. Pfau, A., Sanz, J., Schierbaum, K. D., Göpel, W., Belzunegui, J. P., and Rojo, J. M., *in* "Proceedings 11th International Congress on Catalysis" (J. W. Hightower, W. N. Delgass, E. Iglesias, and A. T. Bell, Eds.), *Stud. Surf. Sci. Catal.* **101**, 931 (1996).
3. Meriaudeau, P., Dutel, J. F., Dufaux, M., and Naccache, C., *Stud. Surf. Sci. Catal.* **11**, 95 (1982).
4. Meriaudeau, P., Dufaux, M., and Naccache, C., *in* "Strong Metal/Support Interactions," ACS Symposium Series, Vol. 298, p. 118. Am. Chem. Soc., Washington, DC, 1986.
5. Summers, J. C., and Ausen, S. A., *J. Catal.* **58**, 131 (1979).
6. Datye, A. K., Kalakkad, D. S., Yao, M. H., and Smith, D. J., *J. Catal.* **155**, 148 (1995).
7. Cochrane, H. D., Hutchinson, J. L., White, D., Parkinson, G. M., Dupas, C., and Scott, A. J., *Ultramicroscopy* **34**, 10 (1990).
8. Chojnacki, T., Krause, K., and Schmidt, L. D., *J. Catal.* **128**, 161 (1991).
9. Schwartz, J. M., and Schmidt, L. D., *J. Catal.* **138**, 283 (1992).
10. Hardacre, C., Rayment, T., and Lambert, R., *J. Catal.* **158**, 102 (1996).
11. Bernal, S., Botana, F. J., Calvino, J. J., Cifredo, G. A., Pérez Omil, J. A., and Pintado, J. M., *Catal. Today* **28**, 219 (1995).
12. Bernal, S., Botana, F. J., García, R., Kang, Z., López, M. L., Pan, M., Ramírez, F., and Rodríguez-Izquierdo, J. M., *Catal. Today* **2**, 653 (1988).
13. Bernal, S., Botana, F. J., Calvino, J. J., Cifredo, G. A., García, R., and Rodríguez-Izquierdo, J. M., *Ultramicroscopy* **34**, 60 (1990).
14. Bernal, S., Calvino, J. J., Cauqui, M. A., Cifredo, G. A., Jobacho, A., and Rodríguez-Izquierdo, J. M., *Appl. Catal.* **99**, 1 (1993).
15. Bernal, S., Botana, F. J., Calvino, J. J., Cauqui, M. A., Clfredo, G. A., Jobacho, A., Pintado, J. M., and Rodríguez-Izquierdo, J. M., *J. Phys. Chem.* **97**, 4118 (1993).
16. Bernal, S., Blanco, G., Calvino, J. J., Cifredo, G. A., Pérez Omil, J. A., Pintado, J. M., and Varo, A., *Stud. Surf. Sci. Catal.* **82**, 507 (1994).
17. Stadelmann, P., *Ultramicroscopy* **21**, 131 (1987).
18. Botana, F. J., Calvino, J. J., Blanco, G., Marcos, M., and Pérez Omil, J. A., "13th International Congress on Electron Microscopy (ICEM13), París, France," abstracts, p. 1085, 1994.
19. Bronger, W., *J. Less-Common Metals* **12**, 63 (1967).
20. Le Roy, J., Moreau, J. M., and Paccard, D., *Acta Crystallogr.* **B34**, 9 (1978).
21. Compton, V. B., and Matthias, B. T., *Acta Crystallogr.* **12**, 651 (1959).
22. Le Roy, J., Moreau, J. M., and Paccard, D., *Acta Crystallogr.* **B33**, 2414 (1977).
23. Dwight, A. E., Conner, R. A., Downey, J. R., and Downey, J. W., *Acta Crystallogr.* **18**, 835 (1985).
24. Botana, F. J., Calvino, J. J., Cifredo, G. A., Pérez Omil, J. A., and Varo, A., "Tenth European Congress on Electron Microscopy (EUREM92), Granada, Spain," abstracts, Vol. 2, p. 387, 1992.
25. Kleykamp, H., *J. Nuclear Mater.* **201**, 193 (1993).